

# Electric conductivity of hot and dense quark matter in a magnetic field with Landau level resummation via kinetic equations

Kenji Fukushima

*Department of Physics, The University of Tokyo,  
7-3-1 Hongo, Bunkyo-ku, Tokyo 113-0033, Japan*

Yoshimasa Hidaka

*Theoretical Research Division, Nishina Center, RIKEN,  
2-1 Hirosawa, Wako, Saitama 351-0198, Japan and  
iTHEMS Program, RIKEN, 2-1 Hirosawa, Wako, Saitama 351-0198, Japan*

We compute the electric conductivity of quark matter at finite temperature  $T$  and quark chemical potential  $\mu$  under a magnetic field  $B$  beyond the Lowest Landau level approximation. The electric conductivity transverse to  $B$  is dominated by the Hall conductivity  $\sigma_H$ . For the longitudinal conductivity  $\sigma_{\parallel}$ , we need to solve kinetic equations. Then, we numerically find that  $\sigma_{\parallel}$  has only mild dependence on  $\mu$  and the quark mass  $m_q$ . Moreover,  $\sigma_{\parallel}$  first decreases and then linearly increases as a function of  $B$ , leading to an intermediate  $B$  region which looks consistent with the experimental signature for the chiral magnetic effect. We also point out that  $\sigma_{\parallel}$  at nonzero  $B$  remains within the range of the lattice-QCD estimate at  $B = 0$ .

PACS numbers: 25.75.-q, 25.75.Nq, 21.65.Qr, 12.38.-t

*Introduction:* Extreme matter of quarks and gluons in quantum chromodynamics (QCD) could realize as a quark-gluon plasma at high energy in nucleus-nucleus collisions and as quark matter at high baryon density in the neutron star cores. Nowadays, the nucleus-nucleus collision experiment is aiming to explore the QCD phase diagram at finite temperature  $T$  and quark chemical potential  $\mu$ , which is called the beam energy scan program. Interestingly, such hot and dense QCD matter may be exposed under a strong magnetic field  $B$  if the nucleus-nucleus collision is noncentral. The presence of strong  $B$  provides us with an ideal probe to topological contents of the QCD vacuum, as exemplified by the chiral magnetic effect (CME) [1] for instance.

To quantify topological effects induced by  $B$ , we need to estimate transport coefficients, among which one of most important is the electric conductivity  $\sigma$ . Indeed, the CME signature in condensed-matter system of Weyl semimetals is the negative magnetoresistance, that is, quadratic rise of  $\sigma_{\text{CME}}(B) \propto B^2$  [2], which has been first detected experimentally in Ref. [3] under an assumption that nontopological  $\sigma$  is insensitive to  $B$ . In contrast to condensed-matter system, for hot and dense quark matter, we can make a first-principles estimate for  $\sigma(B)$  from QCD directly. On top of that  $\sigma(B)$  is an essential parameter for the CME detectability in the nucleus-nucleus collision,  $\sigma(B)$  controls the life time of  $B$  [4, 5].

So far,  $\sigma(B)$  has been perturbatively calculated in QCD under a hierarchy of relevant scales,  $\sqrt{eB} \gg T \gg gT$ , where  $e$  represents the charge of the proton and  $g$  the QCD charge, using the lowest Landau level approximation (LLLA) [6, 7]. Usually, the LLLA is a reasonable approximation for strong  $B$  and has been adopted for various QCD observables such as the heavy quark diffu-

sion constant [8], the bulk viscosity [9], etc. The validity of the LLLA is questionable, however, for  $\sigma(B)$  involving ( $u$  and  $d$ ) quarks with small mass  $m_q$ , i.e.,  $\sigma \rightarrow \infty$  as  $m_q \rightarrow 0$  since the scattering phase space is too severely restricted by the approximation.

In the present work we significantly revise the calculation of  $\sigma(B)$  in a different (more realistic) regime,  $\sqrt{eB} \gg gT$ , which is required to justify our neglecting scattering processes for  $T$ -induced quark damping ( $\sim g^2T$ ), namely,  $\Delta\varepsilon \simeq eB/T \gg g^2T$  where  $\Delta\varepsilon$  is an energy gap associated with adjacent Landau levels. Then, we will find that our  $\sigma$  with full Landau level resummation shows much milder  $m_q$  dependence than the LLLA result. We will also see that the  $B$  dependence is minor. Thus, comparing our finite- $B$   $\sigma$  to the lattice-QCD measured value at  $B = 0$  [10–12] would make sense as a consistency check.

*Some definitions:* The electric conductivity is given by the following Kubo formula:

$$\sigma^{ij} = \lim_{k_0 \rightarrow 0} \lim_{\mathbf{k} \rightarrow \mathbf{0}} \frac{1}{2ik_0} [\Pi_R^{ij}(k) - \Pi_A^{ij}(k)], \quad (1)$$

where  $\Pi_R^{\mu\nu}(k)$  and  $\Pi_A^{\mu\nu}(k)$  are the retarded and the advanced polarization functions, respectively, defined by

$$\Pi_{R/A}^{ij}(k) := \pm i \int d^4x e^{ik \cdot x} \theta(\pm t) \langle [j^i(x), j^j(0)] \rangle, \quad (2)$$

where “+” is for  $R$  and “−” is for  $A$ . We note that, when we work at finite density,  $j^i$  in the above formula is not necessarily the electric current,  $j_{\text{em}}^i = \sum_f q_f \bar{\psi}_f \gamma^i \psi_f$  where  $f$  refers to flavor and  $q_f$  is the electric charge of  $f$ -quark, i.e.,  $q_u = (2/3)e$  and  $q_d = -(1/3)e$ . The hydrodynamic mode subtraction is needed as  $j^i = j_{\text{em}}^i - n_e T^{0i} / (\mathcal{E} + \mathcal{P}_i)$

with the electric charge density  $n_e$ , the energy momentum tensor  $T^{\mu\nu}$ , the energy density  $\mathcal{E} = \langle T^{00} \rangle$ , and the pressure  $\mathcal{P}_i = \langle T^{ii} \rangle$  [13].

For perturbative calculations of  $\Pi_{R/A}^{ij}(k)$  the free quark propagator at finite  $B$  is the essential building block. The retarded propagator in flavor  $f$  sector is given by a sum over the Landau levels labeled by  $n$  as

$$S_{R/A}^f(p) = \sum_{n=0}^{\infty} \frac{-S_n^f(p)}{p_0^2 - \varepsilon_{fn}^2 \pm i\epsilon p_0} = \sum_{n=0}^{\infty} \frac{-S_n^f(p)}{p_{\parallel}^2 - m_{fn}^2 \pm i\epsilon p_0}, \quad (3)$$

where the (flavored) Landau quantized energy dispersion is  $\varepsilon_{fn} = \sqrt{p_z^2 + 2|q_f B|n + m_f^2}$  and we defined  $m_{fn}^2 := 2|q_f B|n + m_f^2$ ,  $p_{\perp}^{\mu} := (0, p_x, p_y, 0)$ , and  $p_{\parallel}^{\mu} := (p_0, 0, 0, p_z)$ . Here, we chose the  $B$  direction along the  $z$  axis without loss of generality. The numerator  $S_n^f(p)$  has Dirac index structures decomposed as

$$S_n^f(p) = (\not{p}_{\parallel} + m) [P_+^f A_n(4\xi_p^f) + P_-^f A_{n-1}(4\xi_p^f)] + \not{p}_{\perp} B_n(4\xi_p^f) \quad (4)$$

with  $\xi_p^f := |\mathbf{p}_{\perp}|^2 / (2|q_f B|)$ . We introduced  $A_n(x) := 2e^{-x/2} (-1)^n L_n(x)$ , and  $B_n(x) := 4e^{-x/2} (-1)^{n-1} L_{n-1}^{(1)}(x)$  where  $L_n(x) = L_n^{(0)}(x)$  and  $L_n^{(\alpha)}(x)$  represent the generalized Laguerre Polynomials [14]. In the above expression  $P_{\pm}^f$  represents the projection operator,  $P_{\pm}^f := (1 \pm \text{sgn}(q_f B) i\gamma^1 \gamma^2) / 2$ .

We adopt the real-time Schwinger-Keldysh formalism in the  $R/A$  basis in which the standard propagators on the Schwinger-Keldysh paths (1,2) are transformed through the following relations:  $S_{RA}^f = -iS_{R'}^f$ ,  $S_{AR}^f = -iS_A^f$ ,  $S_{AA}^f = 0$ , and  $S_{RR}^f = -i[1/2 - n_F(p_0 - \mu_f)](S_R^f - S_A^f)$ , where  $n_F$  is the Fermi-Dirac distribution function.

*Electric conductivity:* We are now ready for proceeding to the conductivity calculation. We decompose the anisotropic tensor structure of the electric conductivity using  $\hat{B}^i := B^i / |\mathbf{B}|$  as

$$\sigma^{ij} = \sigma_H \epsilon^{ijk} \hat{B}^k + \sigma_{\parallel} \hat{B}^i \hat{B}^j + \sigma_{\perp} (\delta^{ij} - \hat{B}^i \hat{B}^j), \quad (5)$$

where  $\sigma_H$  represents the Hall conductivity for an electric current perpendicular to both electric and magnetic fields. In the  $R/A$  basis, the polarization tensor at the one-loop order reads

$$\begin{aligned} \Pi_R^{\mu\nu}(k) &= -i \sum_f q_f^2 \int \frac{d^4 p}{(2\pi)^4} \text{tr} [\gamma^{\mu} S_{RR}^f(k+p) \gamma^{\nu} S_{AR}^f(p)] \\ &\quad - i \sum_f q_f^2 \int \frac{d^4 p}{(2\pi)^4} \text{tr} [\gamma^{\mu} S_{RA}^f(k+p) \gamma^{\nu} S_{RR}^f(p)], \end{aligned} \quad (6)$$

apart from the hydrodynamic mode subtraction, which will be taken into account later. We can straightforwardly perform the integration (6) to get

$$\sigma_H = \frac{n_e}{B}, \quad (7)$$

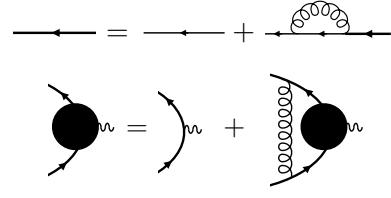


FIG. 1. Illustration of the Bethe-Salpeter equations; the resummed propagator with self-energy insertions (top) and the resummed vertex with ladder diagrams (bottom).

which is nothing but the formula for the Hall conductivity. Up to the one-loop order  $\sigma_{\perp} = 0$  which is intuitively understood from the Landau quantization of transverse motion. A nonzero value of  $\sigma_{\perp}$  appears from the two-loop and higher order contributions. Here, we just give a parametric estimate, that is,

$$\frac{\sigma_{\perp}}{T} \sim \frac{g^2 T^2}{|eB|}, \quad (8)$$

which is small in our condition of  $\sqrt{|eB|} \gg gT$ . This parametric form is derived from one self-energy insertion to the fermion propagators. The leading behavior of the self-energy is  $\sim g^2 T$ , while the propagator is of order  $1/\Delta\varepsilon \sim T/|eB|$ . Thus, the combination of these factors leads to  $g^2 T \cdot T/|eB| = g^2 T^2/|eB| \ll 1$ .

*Kinetic equations:* Next, we calculate the longitudinal conductivity which is of our main interest. To this end we must deal with the resummation over pinching singularities (see Ref. [15] for example). An efficient approach to resum higher order diagrams is solving the Bethe-Salpeter equations, as illustrated in Fig. 1, which amounts to the common formalism used in Ref. [16].

The Bethe-Salpeter equations can be translated to the linearized kinetic or Boltzmann equations, that is,

$$\begin{aligned} 2P_p^{\mu} (\partial_{\mu} + q_f F_{\nu\mu} \partial_{p\nu}) f_p &= -C[f] \\ 2\bar{P}_{p'}^{\mu} (\partial_{\mu} - q_f F_{\nu\mu} \partial_{p'\nu}) \bar{f}_{p'} &= -\bar{C}[f] \\ 2k^{\mu} \partial_{\mu} g_k &= -\tilde{C}[f] \end{aligned} \quad (9)$$

for quarks, anti-quarks, and gluons, respectively, where  $\partial_{p\nu} := \partial/\partial p_{\nu}$  and  $C[f]$ ,  $\bar{C}[f]$ , and  $\tilde{C}[f]$  represent the collision terms. In the above,  $2P_p^{\mu} := \bar{u}(p)\gamma^{\mu}u(p)$  and  $2\bar{P}_{p'}^{\mu} := \bar{v}(p')\gamma^{\mu}v(p')$ , with the wave functions  $u(p)$  and  $v(p')$  for particle and anti-particle, respectively, and the subscript  $p$ ,  $p'$ , and  $k$  represent not only the momenta but also the Landau level  $n$ , the angular momentum  $l$ , the spin  $s$ , the color  $c$ , and the flavor  $f$  collectively.

To solve the Boltzmann equation perturbatively, we expand the distribution functions in terms of small deviations,  $\delta f_p$ ,  $\delta \bar{f}_{p'}$ , and  $\delta g_k$ , around the thermal equilibrium,  $f_{\text{eq}}(p) = n_F(\varepsilon_{fn} - \mu)$ ,  $\bar{f}_{\text{eq}}(p) = n_F(\varepsilon_{fn} + \mu)$ , and  $g_{\text{eq}}(k) = n_B(\omega_k)$  where  $n_B$  is the Bose-Einstein distribution function and  $\omega_k = |\mathbf{k}|$  is the energy of massless gluons. It would be more convenient to introduce  $\chi_p$ ,  $\bar{\chi}_{p'}$ ,

and  $\tilde{\chi}_k$  rescaled by common factors as  $\delta f_p = \beta f_{\text{eq}}(p)[1 - f_{\text{eq}}(p)] E_z \chi_p$ ,  $\delta f_{p'} = \beta f_{\text{eq}}(p')[1 - f_{\text{eq}}(p')] E_z \tilde{\chi}_{p'}$ , and  $\delta g_k = \beta g_{\text{eq}}(k)[1 + g_{\text{eq}}(k)] E_z \tilde{\chi}_k$ , where  $\beta = 1/T$  is the inverse temperature.

Suppose that we solved  $\chi_p$ ,  $\tilde{\chi}_{p'}$ , and  $\tilde{\chi}_k$  from the kinetic equations (9), we can express the electric current as  $j_z = \sigma_{\parallel} E_z = \int_p 2P_p^3 q_f (\delta f_p - \delta \tilde{f}_p)$ , from which we can read  $\sigma_{\parallel}$ , where  $\int$  denotes the phase space sum of all quantum numbers and the invariant integration of momentum. In this way we come by the following formula,

$$\sigma_{\parallel} = \beta N_c \sum_f \frac{q_f |q_f B|}{2\pi} \sum_{n=0}^{\infty} \alpha_n \int \frac{dp_z}{2\pi} \frac{p_z}{\varepsilon_{fn}} \times \left\{ f_{\text{eq}}(p)[1 - f_{\text{eq}}(p)] \chi_p - \bar{f}_{\text{eq}}(p)[1 - \bar{f}_{\text{eq}}(p)] \tilde{\chi}_p \right\}. \quad (10)$$

Here, we introduced the spin degeneracy factor  $\alpha_n$  by  $\alpha_0 = 1$  and  $\alpha_{n>0} = 2$ .

Now, let us return to our problem of solving Eq. (9). In the left-hand side,  $\partial_0$  on  $f_{\text{eq}}$  picks up a term  $\propto \partial_0 u_z$  where  $u_z$  is the  $z$  component of fluid velocity which can be eliminated by the leading order hydrodynamic equation,  $\partial_0 u_z = n_e E_z / (\mathcal{E} + \mathcal{P}_z)$ . Then, the left-hand side of the first equation for quarks simplifies as

$$2P_p^0 (\partial_0 + q_f E_z \partial_{p_z}) f_p = -\beta W_p E_z \left( q_f \frac{p_z}{\varepsilon_{fn}} - \frac{n_e p_z}{\mathcal{E} + \mathcal{P}_z} \right). \quad (11)$$

Here, we defined  $W_p := 2P_p^0 f_{\text{eq}}(p)[1 - f_{\text{eq}}(p)]$ . The second kinetic equation for  $\tilde{f}_p$  has the same structure as above with  $f_p$ ,  $W_p$ , and  $q_f$  replaced with  $\tilde{f}_p$ ,  $\bar{W}_p := 2P_p^0 \bar{f}_{\text{eq}}(p)[1 - \bar{f}_{\text{eq}}(p)]$ , and  $-q_f$ . Likewise, the gluon equation is  $2\omega_k \partial_0 g_k = -\beta \tilde{W}_k (-k_z \partial_0 u_z)$  with  $\tilde{W}_k := 2\omega_k g_{\text{eq}}(k)[1 + g_{\text{eq}}(k)]$ .

Using the following multi-component symbols,

$$\mathcal{J}^{\mu} := q_f \begin{pmatrix} p^{\mu}/\varepsilon_{fn} \\ -p^{\mu}/\varepsilon_{fn'} \\ 0 \end{pmatrix}, \quad \mathcal{T}^{0\mu} := \begin{pmatrix} p^{\mu} \\ p^{\mu} \\ k^{\mu} \end{pmatrix}, \quad (12)$$

we can summarize three kinetic equations as

$$\mathcal{S} := \mathcal{J}^z - \frac{n_e \mathcal{T}^{0z}}{\mathcal{E} + \mathcal{P}_z} = \mathcal{L} \chi, \quad (13)$$

where the left-hand side will be denoted by  $\mathcal{S}$  in what follows, and the right-hand side represents the collision terms;  $\mathcal{L}$  is a linear operator defined by

$$\mathcal{L} \chi := \mathcal{L} \begin{pmatrix} \chi_p \\ \tilde{\chi}_{p'} \\ \tilde{\chi}_k \end{pmatrix} = \frac{1}{\beta E_z} \begin{pmatrix} C[f]/W_p \\ \bar{C}[f]/\bar{W}_{p'} \\ \tilde{C}[f]/\tilde{W}_k \end{pmatrix}. \quad (14)$$

We should then solve  $\chi = \mathcal{L}^{-1} \mathcal{S}$  using our symbolic notation. We note that  $\mathcal{L}$  contains five zero eigenvalues (for a single flavor and more for multi flavors) with the eigenvectors,  $\mathcal{C}^a = \{\mathcal{J}^0, \mathcal{T}^{0\mu}\}$ , corresponding to the charge and

the energy-momentum conservations. For two flavors  $\mathcal{C}^a$  also contains the quark number conservation.

To formulate the projection procedure, let us introduce an inner product for two functions,  $A = (a_p, \bar{a}_{p'}, \tilde{a}_k)$  and  $B = (b_p, \bar{b}_{p'}, \tilde{b}_k)$ , as follows

$$(A, B) := \int_p W_p a_p b_p + \int_{p'} \bar{W}_{p'} \bar{a}_{p'} \bar{b}_{p'} + \int_k \tilde{W}_k \tilde{a}_k \tilde{b}_k. \quad (15)$$

It is then easy to rewrite Eq. (10) as  $\sigma_{\parallel} = \beta (\mathcal{J}^z, \chi)$  using Eq. (12). Now, with the zero eigenvectors  $\mathcal{C}$  and the inner product, we define a projection operator onto functional space excluding zero eigenvalues as

$$\mathcal{Q}O := O - \sum_{a,b} \mathcal{C}^a (\mathcal{C}, \mathcal{C})_{ab}^{-1} (\mathcal{C}^b, O), \quad (16)$$

where  $(\mathcal{C}, \mathcal{C})_{ab}^{-1}$  is the inverse matrix of  $(\mathcal{C}^a, \mathcal{C}^b)$ . We see  $\mathcal{Q}^2 = \mathcal{Q}$  and  $\mathcal{Q}\mathcal{C}^a = 0$  by construction. Using alternative expressions for the charge density and the enthalpy, i.e.,  $n_e = \beta (\mathcal{T}^{0z}, \mathcal{J}^z)$  and  $\mathcal{E} + \mathcal{P}_z = \beta (\mathcal{T}^{0z}, \mathcal{T}^{0z})$  [17], we can write  $\mathcal{S} = \mathcal{Q}\mathcal{J}^z$ . Noting  $\mathcal{L} = \mathcal{L}\mathcal{Q}$ , we find the formal solution of  $\mathcal{L}\chi = \mathcal{S}$  as  $\chi = \mathcal{Q}\mathcal{L}^{-1}\mathcal{Q}\mathcal{S}$ , where  $\mathcal{Q}\mathcal{L}^{-1}\mathcal{Q}$  satisfies a relation  $\mathcal{L}\mathcal{Q}\mathcal{L}^{-1}\mathcal{Q} = \mathcal{Q}$ . We eventually obtain

$$\sigma_{\parallel} = \beta (\mathcal{J}^z, \mathcal{Q}\mathcal{L}^{-1}\mathcal{Q}\mathcal{S}) = \beta (\mathcal{S}, \mathcal{L}^{-1}\mathcal{S}). \quad (17)$$

This means, the zero modes of  $\mathcal{L}$  are already projected out once applied on  $\mathcal{S}$ .

*Collision terms:* The collision term is the most complicated part of our calculations. For  $\sqrt{eB} \gg gT$ , the  $1 \leftrightarrow 2$  process of typical scale  $\sim g^2 eB/T^2$  is dominant as compared to the  $2 \leftrightarrow 2$  process of typical scale  $\sim g^4$ . For the  $1 \leftrightarrow 2$  process there are three distinct contributions,

$$C[f] = C_{q \rightarrow qg}[f] + C_{qg \rightarrow q}[f] + C_{q\bar{q} \rightarrow g}[f], \quad (18)$$

where the subscripts represent processes illustrated in Fig. 2. We can also consider similar decompositions for  $\bar{C}$  for anti-quarks and  $\tilde{C}$  for gluons.

The collision terms take a standard expression in terms of distribution functions and the scattering amplitude. After tedious calculations we find that the scattering amplitudes of the synchrotron radiation and the pair annihilation processes,  $i\mathcal{M}_{p \rightarrow k+p'} = ig \bar{u}(p') \gamma^{\mu} t_a u(p) \varepsilon_{\mu}^*(k)$  and  $i\mathcal{M}_{p+p' \rightarrow k} = ig \bar{v}(p') \gamma^{\mu} t_a u(p) \varepsilon_{\mu}^*(k)$ , can be squared with the summation over the quantum numbers and the phase space, leading to

$$\begin{aligned} & \int_{k,p,p'} |\mathcal{M}_{p \rightarrow p'+k}|^2 (2\pi)^4 \delta^{(4)}(k - p + p') \\ &= -\frac{1}{2} \sum_{f, n, n'} \int \frac{dp_z}{2\pi} \frac{1}{2\varepsilon_{fn}} \int_{p'_z}^{p_z} \frac{dp'_z}{2\pi} \frac{1}{2\varepsilon_{fn'}} X(n, n', \xi_{-}^f), \end{aligned} \quad (19)$$

$$\begin{aligned} & \int_{k,p,p'} |\mathcal{M}_{p+p' \rightarrow k}|^2 (2\pi)^4 \delta^{(4)}(p + p' - k) \\ &= \frac{1}{2} \sum_{f, n, n'} \int \frac{dp_z}{2\pi} \frac{1}{2\varepsilon_{fn}} \int \frac{dp'_z}{2\pi} \frac{1}{2\varepsilon_{fn'}} X(n, n', \xi_{+}^f), \end{aligned} \quad (20)$$

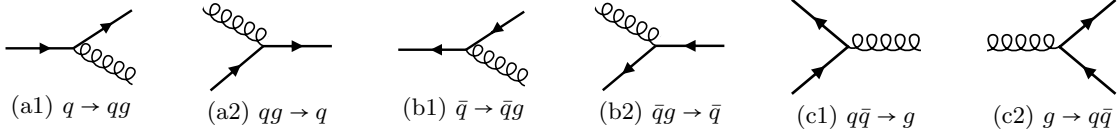


FIG. 2. Diagrams of the synchrotron radiation process with a quark (a1), with an anti-quark (b1), and the pair annihilation (c1). Their inverse processes are (a2), (b2), and (c2), respectively.

where the allowed range of  $p'_z$  is restricted for the synchrotron radiation in Eq. (19) as  $p'_{z-} < p'_z < p'_{z+}$  with

$$p'_{z\pm} = p_z \frac{m_{fn}^2 + m_{fn'}^2}{2m_{fn}^2} \pm \frac{m_{fn}^2 - m_{fn'}^2}{2m_{fn}^2} \sqrt{m_{fn}^2 + p_z^2}. \quad (21)$$

Two integrands in Eqs. (19) and (20) are identical, i.e.,  $X(n, n', \xi_k) := g^2 N_c C_F \int \frac{d^2 p_z}{(2\pi)^2} \text{tr} [\gamma_\mu S_n^f(p) \gamma^\mu S_{n'}^f(p-k)]$  with a group factor  $C_F := (N_c^2 - 1)/(2N_c)$ , except for the kinematical constraint, that is, the argument of  $X(n, n', \xi_\pm^f)$  is given by

$$\xi_\pm^f = \frac{(\varepsilon_{fn} \pm \varepsilon_{fn'})^2 - (p_z \pm p'_z)^2}{2|q_f B|}. \quad (22)$$

Using Eq. (4) and properties of the Laguerre polynomials we find

$$\begin{aligned} X(n, n', \xi) &= g^2 N_c C_F \frac{|q_f B|}{2\pi} e^{-\xi} \frac{n!}{n!} \xi^{n'-n} \left\{ \left[ 4m_f^2 \right. \right. \\ &\quad \left. \left. - 4|q_f B|(n+n'-\xi) \frac{1}{\xi} (n+n') \right] F(n, n', \xi) \right. \\ &\quad \left. + 16|q_f B| n' (n+n') \frac{1}{\xi} L_n^{(n'-n)}(\xi) L_{n-1}^{(n'-n)}(\xi) \right\}, \quad (23) \\ F(n, n', \xi) &:= \begin{cases} 1 & (n=0) \\ \left[ L_n^{(n'-n)}(\xi) \right]^2 + \frac{n'}{n} \left[ L_{n-1}^{(n'-n)}(\xi) \right]^2 & (n>0). \end{cases} \quad (24) \end{aligned}$$

*Recovery of the lowest Landau level approximation:* It would be an instructive check to see that the LLLA result is correctly recovered in the limit of  $eB \gg T^2$  (at  $\mu = 0$ ). Since the synchrotron radiation changes the Landau level, we can safely discard it. For the pair annihilation process,  $X(n=0, n'=0, \xi)$  given in Eq. (23) simplifies as  $X(0, 0, \xi_+^f) = 4m_f^2 g^2 N_c C_F \frac{|q_f B|}{2\pi} e^{-\xi_+^0}$  with  $\xi_+^0 = [(\sqrt{p_z^2 + m_f^2} + \sqrt{p_z'^2 + m_f^2})^2 - (p_z + p_z')^2] / (2|q_f B|)$  which is nothing but  $\xi_+$  in Eq. (22) with  $n = n' = 0$ . When  $|q_f B|$  is much larger than any other scales, we can approximate  $e^{-\xi_+^0} \approx 1$ . Then, the linearized kinetic equations reduce to a simple form as

$$\begin{aligned} q_f N_c \frac{|q_f B|}{2\pi} \beta f_{\text{eq}}(p) [1 - f_{\text{eq}}(p)] \frac{p_z}{\varepsilon_{f0}} &= 4m_f^2 g^2 N_c C_F \\ \times \beta \frac{|q_f B|}{2\pi} \cdot \frac{1}{4\varepsilon_{f0}} \int \frac{dp'_z}{2\pi} \frac{1}{2\varepsilon'_{f0}} f_{\text{eq}}(p) \bar{f}_{\text{eq}}(p') [1 + g_{\text{eq}}(k)] \chi_p, \quad (25) \end{aligned}$$

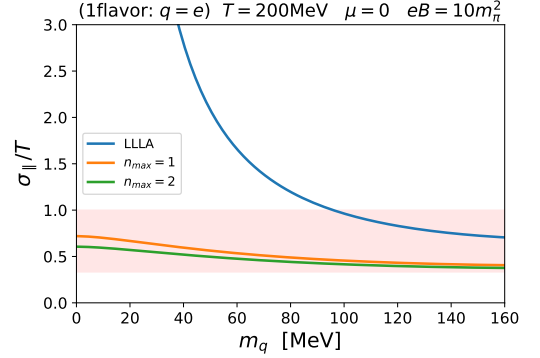


FIG. 3. Mass dependence of  $\sigma_{\parallel}$  for single flavor at  $T = 200 \text{ MeV}$ ,  $\mu = 0$ ,  $eB = 10m_\pi^2$ , and  $g^2/(4\pi) = 0.3$ . The shaded region is the lattice-QCD estimate from Ref. [11].

where  $\varepsilon_{f0} = \sqrt{p_z^2 + m_f^2}$  and  $\varepsilon'_{f0} = \sqrt{p_z'^2 + m_f^2}$ . Here we do not have to consider mixing terms with  $\bar{\chi}_{p'}$ . In this special limit,  $\mathcal{L}$  is not really a matrix and we do not need to take its matrix inversion. Actually, we can easily solve the above kinetic equation to obtain  $\chi_p$ . Thanks to the charge conjugation symmetry, the solution for anti-quarks is  $\bar{\chi}_p = -\chi_p$ . Summarizing them, we finally arrive at the LLLA result from Eq. (17) as

$$\begin{aligned} \sigma_{\parallel} &= \sum_f \frac{N_c \beta}{g^2 C_F m_f^2} q_f^2 \frac{|q_f B|}{2\pi} \int \frac{dp_z}{2\pi} \frac{p_z^2}{\varepsilon_{f0}} \\ &\quad \times \frac{f_{\text{eq}}(p) [1 - f_{\text{eq}}(p)]^2}{\int \frac{dp'_z}{2\pi} \frac{1}{\varepsilon'_{f0}} \bar{f}_{\text{eq}}(p') [1 + g_{\text{eq}}(k)]}, \quad (26) \end{aligned}$$

which is consistent with Ref. [7].

*Numerical results and discussions:* Now we have all necessary ingredients to write down the matrix elements of  $\mathcal{L}$  as a phase space convolution of  $X(n, n', \xi_\pm^f)$  and the distribution functions,  $f_{\text{eq}}$ ,  $\bar{f}_{\text{eq}}$ , and  $g_{\text{eq}}$ . Besides the flavor  $f$  and the Landau level  $n$ , we should choose the complete set basis for functions of  $p_z$ ,  $k_z$  and  $k_{\perp}$ , which we will take the simplest polynomial form as  $\hat{p}_z |p_z|^m$  for (anti-)quarks and  $k_{\perp}^m$  for gluons with integral  $m$ .

Figure 3 shows our numerical results for the quark mass dependence of  $\sigma_{\parallel}/T$  for a fictitious single flavor with  $q = e$  at finite  $T$  and  $B$  but at zero  $\mu$ . We choose that the QCD charge as  $g^2/(4\pi) = 0.3$ . We clearly see that the LLLA has artificial enhancement as  $m_q$  approaches zero.

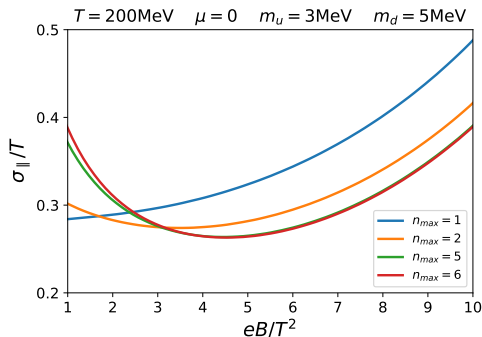


FIG. 4. Magnetic and  $n_{\max}$  dependence of  $\sigma_{\parallel}/T$ .

For the numerical calculation we truncate the Landau level at  $n_{\max}$ . In the  $eB = 10m_{\pi}^2$  case, the convergence of the Landau level sum is very fast and  $n_{\max} = 1$  already gives a good approximation, even though the LLLA badly breaks down in the small  $m_q$  region. It is interesting that our result is quantitatively consistent with the lattice-QCD estimate,  $0.3 \leq \sigma/T \leq 1.0$  (for the quark charge squared sum  $C_{\text{em}} = 1$ ) [11], which is indicated by the shaded region in Fig. 3.

The  $B$  dependence of  $\sigma_{\parallel}/T$  has a nonmonotonic structure as shown in Fig. 4, for which we adopted a physical parameter set with  $u$  and  $d$  quarks. For small  $n_{\max}$  or strong  $B$ , the LLL contribution is dominant, and then  $\sigma_{\parallel}$  is linearly proportional to  $B$  (reflecting the fact that the charge carrier increases), which explains the growing behavior at large  $B$  in Fig. 4. When  $B$  is not such large, contributions from higher Landau levels lead to a larger interaction cross section due to the phase space factor, which pushes  $\sigma_{\parallel}$  down with larger  $B$ . As a result of the interplay of these competing effects, in an intermediate region of  $B$ , the increasing behavior of  $\sigma_{\parallel}$  looks quadratic; moreover, this nonmonotonic behavior is consistent with what is seen in the CME experiment in Ref. [3]. Although quantitative details may depend on underlying theory, qualitative features should be the same for general physical systems (but could be different with different approximations, say, the relaxation time approximation for the collision term [2] may lead to a different  $B$  dependence).

Finally, we discuss the  $\mu$  dependence as shown in Fig. 5. It is surprising at a first glance that  $\sigma_{\parallel}$  is rather insensitive to  $\mu$ . This can be qualitatively understood from the fact that the carrier density is different from the net particle number but is related to the sum of particle and anti-particle numbers. This latter quantity is not much changed by  $\mu$  which causes imbalance between particles and anti-particles. In the future our estimated  $B$  dependence of  $\sigma_{\parallel}$  could be tested by the lattice-QCD simulation at finite  $B$ , while our calculation at finite  $\mu$  would be a unique prediction. The full details of the an-

alytical derivations and the numerical procedures will be

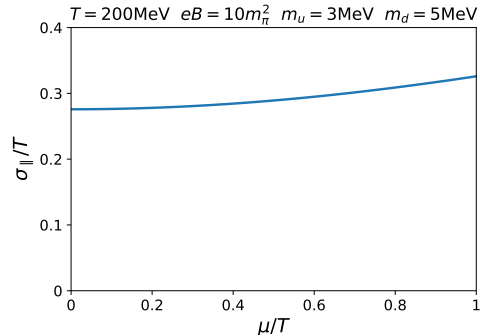


FIG. 5. Density dependence for  $n_{\max} = 2$ .

provided in the follow-up paper.

The authors thank Koichi Hattori, Daisuke Satow, and Misha Stephanov for useful comments and discussions. This work was supported by Japan Society for the Promotion of Science (JSPS) KAKENHI Grant No. 15H03652, 15K13479, and 16K17716.

- 
- [1] K. Fukushima, D. E. Kharzeev, and H. J. Warringa, *Phys. Rev.* **D78**, 074033 (2008).
  - [2] D. T. Son and B. Z. Spivak, *Phys. Rev.* **B88**, 104412 (2013).
  - [3] Q. Li, D. E. Kharzeev, C. Zhang, Y. Huang, I. Pletikoscic, A. V. Fedorov, R. D. Zhong, J. A. Schneeloch, G. D. Gu, and T. Valla, *Nature Phys.* **12**, 550 (2016).
  - [4] L. McLerran and V. Skokov, *Nucl. Phys.* **A929**, 184 (2014).
  - [5] K. Tuchin, *Phys. Rev.* **C93**, 014905 (2016).
  - [6] K. Hattori and D. Satow, *Phys. Rev.* **D94**, 114032 (2016).
  - [7] K. Hattori, S. Li, D. Satow, and H.-U. Yee, *Phys. Rev.* **D95**, 076008 (2017).
  - [8] K. Fukushima, K. Hattori, H.-U. Yee, and Y. Yin, *Phys. Rev.* **D93**, 074028 (2016).
  - [9] K. Hattori, X.-G. Huang, D. H. Rischke, and D. Satow, (2017).
  - [10] G. Aarts, C. Allton, J. Foley, S. Hands, and S. Kim, *Phys. Rev. Lett.* **99**, 022002 (2007).
  - [11] H. T. Ding, A. Francis, O. Kaczmarek, F. Karsch, E. Laermann, and W. Soeldner, *Phys. Rev.* **D83**, 034504 (2011).
  - [12] H.-T. Ding, O. Kaczmarek, and F. Meyer, *Phys. Rev.* **D94**, 034504 (2016).
  - [13] D. N. Zubarev, A. V. Prozorkevich, and S. A. Smolyanskii, *Theor. Math. Phys.* **40**, 821 (1979).
  - [14] V. Gusynin, V. Miransky, and I. Shovkovy, *Phys. Lett.* **B349**, 477 (1995).
  - [15] Y. Hidaka and T. Kunihiro, *Phys. Rev.* **D83**, 076004 (2011).
  - [16] P. B. Arnold, G. D. Moore, and L. G. Yaffe, *JHEP* **11**, 001 (2000).
  - [17] Y. Minami and Y. Hidaka, *Phys. Rev.* **E87**, 023007 (2013).